Developmental Biology 390 (2014) 102–115

Contents lists available at ScienceDirect

Developmental Biology

journal homepage: www.elsevier.com/locate/developmentalbiology

Neuroblast lineage identification and lineage-specific Hox gene action during postembryonic development of the subesophageal ganglion in the *Drosophila* central brain

Philipp A. Kuert [a,*], Volker Hartenstein [b], Bruno C. Bello [a], Jennifer K. Lovick [b], Heinrich Reichert [a]

[a] Biozentrum, University of Basel, Basel, Switzerland
[b] Department of Molecular, Cell and Developmental Biology, University of California, Los Angeles, California, USA

ARTICLE INFO

Article history:
Received 22 November 2013
Received in revised form
23 March 2014
Accepted 29 March 2014
Available online 5 April 2014

Keywords:
Neuroblast
lineage
Hox
Dfd
Scr
Antp

ABSTRACT

The central brain of *Drosophila* consists of the supraesophageal ganglion (SPG) and the subesophageal ganglion (SEG), both of which are generated by neural stem cell-like neuroblasts during embryonic and postembryonic development. Considerable information has been obtained on postembryonic development of the neuroblasts and their lineages in the SPG. In contrast, very little is known about neuroblasts, neural lineages, or any other aspect of the postembryonic development in the SEG. Here we characterize the neuroanatomy of the larval SEG in terms of tracts, commissures, and other landmark features as compared to a thoracic ganglion. We then use clonal MARCM labeling to identify all adult-specific neuroblast lineages in the late larval SEG and find a surprisingly small number of neuroblast lineages, 13 paired and one unpaired. The Hox genes *Dfd*, *Scr*, and *Antp* are expressed in a lineage-specific manner in these lineages during postembryonic development. Hox gene loss-of-function causes lineage-specific defects in axonal targeting and reduction in neural cell numbers. Moreover, it results in the formation of novel ectopic neuroblast lineages. Apoptosis block also results in ectopic lineages suggesting that Hox genes are required for lineage-specific termination of proliferation through programmed cell death. Taken together, our findings show that postembryonic development in the SEG is mediated by a surprisingly small set of identified lineages and requires lineage-specific Hox gene action to ensure the correct formation of adult-specific neurons in the *Drosophila* brain.

Introduction

Neurons of the *Drosophila* central brain and ventral ganglia form lineages that are generated by neural stem cell-like neuroblasts. Neuroblasts segregate from the neuroectoderm of the early embryo (Technau et al., 2006; Urbach and Technau, 2004) and undergo a series of asymmetric divisions, generating the primary neurons that differentiate into the functional CNS of the larva. After a period of quiescence, most neuroblasts resume proliferation to generate the secondary neurons which form the bulk of neurons of the adult CNS. Adult-specific secondary neurons remain immature throughout the larval phase. During metamorphosis, secondary neurons mature and together with reconfigured primary neurons, form the circuits of the adult brain (see Egger et al., 2008; Hartenstein et al., 2008).

Neuroblasts and their lineages have been described in previous work for the ventral ganglia and for the supraesophageal ganglion of the brain. Each ganglion of the ventral nerve cord derives from a set of approximately 30 neuroblast pairs which can be identified based on position, marker expression, and the neuroanatomy of their progeny (Bossing et al., 1996; Doe, 1992; Schmid et al., 1999; Schmidt et al., 1997; Technau et al., 2006). The supraesophageal ganglion (SPG), comprising three modified neuromeres (protocerebrum, deutocerebrum, tritocerebrum), derives from approximately 100 identified neuroblast pairs whose spatial organization and molecular marker expression have also been documented in detail (Urbach and Technau, 2003; Younossi-Hartenstein et al., 1996). Adult-specific secondary lineages of the CNS have been mapped for the ventral ganglia (Truman et al., 2004) and the SPG (Cardona et al., 2009; Ito et al., 2013; Lovick et al., 2013; Pereanu and Hartenstein, 2006; Wong et al., 2013; Yu et al., 2013).

* Corresponding author. Fax: +41 61 267 1613.
E-mail addresses: philipp.kuert@unibas.ch (P.A. Kuert), volkerh@mcdb.ucla.edu (V. Hartenstein), jlovick@ucla.edu (J.K. Lovick), heinrich.reichert@unibas.ch (H. Reichert).

http://dx.doi.org/10.1016/j.ydbio.2014.03.021
0012-1606/

Compared to the wealth of information available for the development of the SPG and ventral ganglia, much less is known about the development of the subesophageal ganglion (SEG), the part of the central brain responsible for feeding behavior and the processing of gustatory information. The SEG derives from three anterior neuromeres of the ventral nerve cord which in all contain approximately 80 pairs of neuroblasts (R. Urbach, personal communication). Similar to neuroblasts of the SPG and ventral ganglia, these cells produce primary and secondary lineages, but to date no information exists regarding location and projection pattern of the SEG neuroblast lineages.

Here we focus on the neuroblasts that generate the adult-specific secondary neurons of the SEG during postembryonic development. We first characterize the general neuroanatomical features of the larval SEG compared to those of a thoracic ganglion. Based on this neuroanatomical analysis, we investigate the adult-specific neuroblast lineages in the SEG and find that a surprisingly small number of lineages, 13 paired and one unpaired lineages, are present at the late larval stage. We use clonal MARCM labeling to identify and characterize each of these lineages individually. We then show that the Hox genes *Deformed* (*Dfd*), *Sex combs reduced* (*Scr*), and *Antennapedia* (*Antp*) are expressed in the postembryonic SEG and demonstrate that most of the SEG lineages express one of these Hox genes. Subsequently, we show that Hox gene inactivation causes lineage-specific axonal targeting defects and neural cell number reduction as well as formation of five ectopic neuroblast lineage types not present in the wildtype brain. Clonal inactivation of apoptosis results in comparable ectopic lineages implying that Hox genes are required for lineage-specific proliferation termination through programmed cell death. Taken together, this report shows that postembryonic development in the SEG is mediated by a small set of neuroblast lineages and requires lineage-specific Hox gene action to ensure the correct formation of adult-specific neurons.

Materials and methods

Genetics

Reporter lines that were used: *act*-GFP^{JMR1} (B.C. Bello)/*Antp*-GFP (H. Bellen)/*engrailed*-Gal4, UAS-H2B::YFP (A. Brand, P. Fichelson, S. Sprecher)/*fasciclin*-GFP (Siebert et al., 2009)/*inscuteable*-Gal4 > UAS-GFP (L. Jan, Y. Jan). For embryonic cell death block experiments was used: Df(3 L)H99, *kni*$^{ri-1}$ p^{p}. For MARCM experiments (Lee and Luo, 1999, 2001), embryos were collected on standard medium over a 4–8 h time window, raised at 25 °C for 24 or 48 h and then heat-shocked for 1 h at 37 °C. Late L3 larvae were picked in the wandering stage. MARCM drivers that were used: hsFLP^{122}; *tub*P-GAL4, UASmCD8::GFP^{LL5}; FRT2A, *tub*PGAL80^{LL9} (B.C. Bello)/hsFLP^{122}; *tub*P-GAL4, UAS-mCD8::GFP^{LL5}; FRT82B, *tub*P-GAL80^{LL5} (B.C. Bello). MARCM responders that were used: FRT2A, Df(3 L)H99, *kni*$^{ri-1}$/FRT82B/FRT82B, *Ki*^{1}, *Dfd*^{12}, p^{p} (B.C. Bello)/FRT82B, *Ki*^{1}, *pb*^{5}, *Dfd*^{16}, *e*^{1} (B.C. Bello)/FRT82B, *pb*^{27}, *Scr*^{2}, p^{p}, *cu*, P{w^{+}, ry^{+}}90E (Percival-Smith et al., 1997)/FRT82B, *Scr*^{4}, *Antp*^{25}, p^{p} (B.C. Bello) /FRT82B, *Antp* $^{NS+RC3}$, *e* (B.C. Bello).

Immunohistochemistry

Embryos and larval brains were fixed and labeled as previously described (Patel, 1994; Pereanu, Hartenstein, 2006; Bello et al., 2007). Primary antibodies: guinea pig-anti-Deadpan (1:500 or 1:1000; gift from J. Skeath), guinea pig-anti-Deformed (1:200; gift from W. McGinnis), guinea pig-anti-Hey (1:1000; gift from C. Delidakis), mouse-anti-Antennapedia (1:100; Condie et al., 1991), mouse-anti-BP106 Neurotactin (1:10 or 1:20; DSHB), mouse-anti-Engrailed (1:1 or 1:5; DHSB), mouse-anti-nc82 (1:20; DSHB), rabbit-anti-Deformed (1:100; gift from T. Kaufman), rabbit-anti-Labial (1:200; F. Hirth, H. Reichert), rabbit-anti-Sex combs reduced (1:400; LeMotte et al., 1989), rat-anti-N-Cadherin (1:25; DSHB). Alexa (Molecular Probes) and Dylight (KPL) secondary antibodies were used between 1:200 and 1:500.

Microscopy and data processing

Images were recorded using a Leica SP5 or a Zeiss LSM 700 Meta confocal microscope. Optical sections ranged from 1 to 2 μm. Resolution of images were either 512 × 512 or 1024 × 1024 pixel. Collected images were processed and arranged using ImageJ, Fiji, Adobe Photoshop and Adobe Illustrator. Statistical t-tests were made with Microsoft Excel. For highlighting specific MARCM clones, cell bodies and neurites from other lineages in the vicinity were removed in every single optical section. 3D models were generated with Fiji 3D viewer and Bitplane Imaris.

Results

The larval SEG is composed of three neuromeres (mandibular, maxillary, and labial ganglia) each of which represents a reduced/modified version of the thoracic neuromeres described in detail in previous works (Landgraf et al., 2003; Nassif et al., 2003; Pflüger et al., 1988; Power, 1948; Truman et al., 2004; Tyrer and Gregory, 1982). To elucidate the architecture and neuroblast lineage composition of the SEG neuromeres, it is therefore helpful to first establish the relationship between landmark structures and neuroblast lineages for a "prototypical" thoracic neuromere of the larval VNC.

Neuroanatomical landmark structures and neuroblast lineages in thoracic neuromeres of the larval CNS

In each thoracic neuromere, connectives and commissures form a scaffold of landmark structures to which individual neuroblast lineages have been related (Truman et al., 2004). The central part of each larval thoracic neuromere is occupied by the anterior and posterior intermediate commissure (aI, pI; Fig. 1B, E, and F). A set of three connectives, called dorso-medial tract (DMT), dorso-intermediate tract (DIT), and dorso-lateral tract (DLT), extend dorsally of the commissures; another three connectives, the ventro-medial tract (VMT), ventro-intermediate tract (VIT), and ventro-lateral tract (VLT), flank the commissures on their ventral side (Fig. 1A, B, and E). In addition, a pair of thinner commissural bundles crosses the midline dorsally (aD, pD; Fig. 1E and F) and one commissure crosses ventrally (aV; Fig. 1A and E).

Secondary neuroblast lineages of the larval thoracic ganglia are referred to by number from 0 to 24 (Brierley et al., 2012; Truman et al., 2004). The secondary axon tracts (SATs) of these lineages enter the neuropil in bundles of 3–4 at characteristic positions. As shown in Fig. 1C and D, the points of entry of these bundles form conspicuous, metamerically reiterated indentations ("portals") at the neuropil surface. Four lineages, 5, 6, 3, and 12, enter vertically through the posterior-medial portal (PMP; Fig. 1D and F). The SATs of lineages 5, 6, 12 turn medially and cross the pI commissure while a second SAT branch of lineages 6 and 12, as well as the lineage 3 SAT, turn laterally towards the dorsal neuropil, forming the posterior vertical tract (pVT; Fig. 1F). A dorsal branch of lineage 6 constitutes the posterior dorsal commissure (pD; Fig. 1F). The SATs of three lineages (11, 19, 23) enter the neuropil through the posterior lateral portal (PLP) and extend medially towards (11) or across (19, 23) the posterior intermediate commissure (Fig. 1D and F).

In the anterior half of each thoracic neuromere four lineages (7, 8, 15, and 16) form a group of SATs that enter the neuropil through the anterior lateral portal (ALP; Fig. 1A, C, D, and E). SATs of lineages 7 and

8 project medially and cross in the anterior intermediate commissure (aI; Fig. 1E). SATs of lineages 15 and 16 branch in the leg neuropil. Lineages 9, 17, and 18 form a "lateral triplet" (Truman et al., 2004), entering the anterior-lateral cortex and projecting medially in the anterior-ventral (aV) or anterior intermediate (aI) commissure (Fig. 1D and E). A posterior triplet of lineages (20–22) project superficially into the posterior surface of the ventrolateral neuropil(Fig. 1F).

SATs of seven further lineages (0, 1, 2, 4, 10, 13, and 14) enter the neuropil as individual tracts. The SAT of lineage 1 contributes to the anterior intermediate commissure (aI) of the posteriorly adjacent neuromere (Fig. 1F and H). SATs of lineages, 4, 13 and 14 contribute to the ventral commissure (aV); the SAT of lineage 10 contributes to the anterior intermediate commissure (aI), and the SAT of lineage 2 projects ipsilaterally along the anterior dorsal (aD) commissure (Fig. 1E). Lineage 0 is the only unpaired lineage; its tract extends vertically into the posterior intermediate (pI) commissure (Fig. 1. D and F).

Neuroanatomical landmark structures and secondary axon tracts in the neuromeres of the larval SEG

The metameric architecture described above for the thoracic neuromeres is also apparent in the SEG, albeit in a substantially modified form (Fig. 1A and B). The SEG can be divided into the labium and the subesophageal anterior (SA) domain, which comprises the mandibular and maxillary neuromeres. As in the thoracic neuromeres, the paired connectives flank a set of intermediate commissures. A fully formed pI commissure (pI_{LB}; Fig. 1B) is formed in the posterior SEG, which is occupied by the labium. This neuromere comprises nine SATs which correspond to SATs in the thoracic neuromeres and are therefore numbered accordingly (Truman et al., 2004).

Two groups of paired SATs enter the posterior SEG through a postero-medial portal (PMP_{LB}; 3, 5, 6, 12) and postero-lateral portal (PLP_{LB}; 11, 19, 23), and an unpaired SAT (0) projects vertically in the midline (Fig. 1D and H). In front of the pI_{LB} commissure, two additional commissures, aI_{LB} and I_{SA}, are present (Fig. 1B). One SAT (7) forms the aI_{LB} commissure (Fig. 1G).

The SA domain manifests a single commissure, I_{SA}, and five SATs. The anterior and posterior portal of the anterior subesophageal ganglion (aSAP, pSAP) continue the metameric series of neuropil portals (arrows in Fig. 1A, C, and D). Two SATs (SA4, SA5) enter through the pSAP, (Fig. 1C, D, and J). Two SATs (SA1, SA2) enter through the aSAP (Fig. 1C, D, and I). One SAT (SA3) enters close to the aSAP, but projects posteriorly and medially, forming the anterior-most commissure (I_{SA}; Fig. 1I and J).

This characterization of the SEG indicates that a remarkably small number of individually identifiable SATs are found in the SEG neuropil. Thus, 13 different bilaterally symmetrical SAT pairs and one unpaired midline SAT are manifest in the neuromeres of the larval SEG.

To confirm that each of the SATs in the larval SEG derives from one neuroblast lineage, we performed a MARCM-based clonal analysis (Lee and Luo, 1999, 2001). Randomly labeled clones with a ubiquitous *tubulin*-Gal4 driving UAS-mCD8::GFP were induced in early larval stages and recovered in the late larval brain (100 specimens). We identified a total of 14 different neuroblast clone types in the postembryonic SEG (summarized in Fig. 4, Fig. 6P, and Table S3). Based on cell body position and SAT trajectory, each of these 14 different MARCM neuroblast clones corresponds unambiguously to one of the 14 SAT types that were found to comprise the larval SEG. A total of 9 SEG lineages in the labial neuromere can be individually identified and homologized with thoracic lineages based on neuropil entry point or projection pattern within the neuropil. These are shown in horizontal and vertical projections in Fig. 2 and S1. Five further identified lineages located anterior to the labial neuromere cannot be homologized with thoracic lineages based on neuroanatomy; we refer to these lineages as SA1-5. They are shown in horizontal and vertical projections in Fig. 3. A characterization of each of these 14 neuroblast lineages is presented below. (Beside these lineages,

Fig. 1. Neuroanatomical landmarks of the larval ventral nerve cord. (A and B) Z-projections of contiguous confocal sections of 3rd instar ventral nerve cord (vnc) labeled with BP106 Neurotactin (red), FasII (green), and DNcad (blue). The plane of sectioning is parallel to the length axis of the ventral nerve cord. Both z-projections represent slices of approximately 20 μm thickness. (A) shows the ventral neuropil (40–60 μm from the ventral surface of the vnc) and (B) the central neuropil (60–80 μm from the ventral surface). Only the anterior part of the ventral nerve cord and adjoining brain, including the neuromeres of the tritocerebrum (TR), subesophageal ganglion [SA anterior subesophageal ganglion, formed by two contracted neuromeres (MX maxilla, MD mandible); LB labium] and the first two thoracic neuromeres (T1 and T2) are shown. Anterior is to the top. Illustrated in (A) are the ventral longitudinal connectives (FasII-positive; green; VMT ventro-medial tract; VIT ventro-intermediate tract), the ventral commissures of the thoracic neuromeres (BP106-positive; red; aV_{T1}, aV_{T2}), the primordia of the leg neuropils (LN) of the thoracic neuromeres, and the entry portals of secondary lineages (hatched lines; ALP antero-lateral portal; PLP postero-lateral portal; PMP postero-medial portal). Approximate neuromere boundaries are indicated by horizontal lines. Segmental nerves (FasII-positive) are rendered yellow ($SN_{LB\ MX}$ fused segmental nerve of the subesophageal ganglion=labio-maxillary nerve; SN_{T1} segmental nerve of T1 neuromere; SN_{T2} segmental nerve of T2 neuromere). Asterisk marks anterior (maxillary) root of the labio-maxillary nerve, arrowhead points out posterior (labial) root of the same nerve. Shown in (B) are the set of dorsal connectives (FasII-positive; green; DMT dorso-medial tract; DIT dorso-intermediate tract; DLT dorso-lateral tract), and the intermediate commissures (BP106-positive; red). Thoracic neuromeres each have a pair of intermediate commissures (aI_{T1} anterior intermediate commissure of T1; pI_{T1} posterior intermediate commissure of T1; aI_{T2} anterior intermediate commissure of T2; pI_{T2} posterior intermediate commissure of T2). Two commissures are also present in the labial neuromere (aI_{LB}, pI_{LB}). The anterior part of the subesophageal ganglion (SA) has but a single BP106-positive commissure (I_{SA}). (C) Volume-rendering of a series of confocal sections of larval ventral nerve cord labeled with DNcad, showing surface topography of neuropil. Small arrows point at transverse fissures in between neuromeres (LB labial neuromere; MD mandibular neuromere; MX maxillary neuromere; T1/T2 thoracic neuromeres 1/2; TR tritocerebrum). Entry portals of secondary lineages are marked by depressions in the ventral neuropil surface [blue hatched lines: postero-medial portals (PMP) and anterior/posterior portal of the anterior subesophageal ganglion (aSAP/pSAP); purple hatched lines: postero-lateral portals (PLP); yellow hatched lines: antero-lateral portals (ALP)]. (D) Z-projection of confocal sections of ventral nerve cord labeled with *insc*-Gal4 (red) and Nc82 (green), corresponding to a slice 40–50 μm from the ventral surface. Hatched lines indicate entry portals of secondary lineages; *insc*-Gal4-positive secondary lineage tracts (red) enter into a Nc82-negative "cavity" which constitutes the portal. Individual lineages are indicated by numbers underneath or next to their corresponding entry portal. (E–J) Z-projections of digitally rotated confocal sections of ventral nerve cord labeled with BP106 (red), FasII (green) and DNcad (blue). Panels show slices of the nerve cord of approximately 20 μm thickness. Dorsal is to the top. Antero-posterior levels of slices is indicated by boxed capital letters ("E–J") to the right of panel B. Panels E and F correspond to an anterior and posterior level of the first thoracic segment. Note BP106-positive anterior commissures in E (aV_{T1} antero-ventral commissure; aI_{T1} antero-intermediate commissure; aD_{T1} antero-dorsal commissure) and posterior commissures in F (pI_{T1} postero-intermediate commissure; pD_{T1} postero-dorsal commissure). Note also the antero-lateral entry portal (ALP) in panel (E), and the postero-lateral and postero-medial entry portal (PLP, PMP) in (F). The FasII-positive longitudinal tracts flank the intermediate commissures dorsally (DMT, DIT, DLT) and ventrally (VMT, VIT). Secondary lineages, some of them associated with entry portals (PMP, PLP, ALP) are indicated by numbers. Panels (G) and (H) show anterior and posterior level of the labial neuromere; the arrangement of commissures, connectives and secondary lineage trajectories is similar to that in the thoracic neuromeres, excepting ventral structures that are reduced or missing in the labial neuromere; note absence of ventral commissure, leg neuropil, and secondary lineages 9, 13–14, 17–18, 20–22 (among others) associated with ventral structures. Panels (I) and (J) represent slices of the anterior subesophageal ganglion (SA) which consists of two reduced neuromeres. The anterior slice (I) illustrates the level of the anterior entry portal of the SA (aSAP) which contains the tracts of lineages SA1 and SA2; the posterior slice (J) lies at the level of the posterior entry portal of the SA (pSAP) that admits lineages SA4 and SA5. The tract of lineage SA3 forms an intermediate commissure (I_{SA}), representing the anterior-most of the three BP106-positive commissures of the SEG (see panel B). Other abbreviations: AP anterior pillar; IP intermediate pillar; LT lateral triplet (lineages 9, 17, 18); PP posterior pillar; PT posterior triplet (lineages 20–22); pVA_{T1} posterior ventral arch of T1; $pVLA_{T1}$ posterior ventro-lateral arch of T1. (A–D) ventral view; (E–J) posterior view. Scale bars: 30 μm.

small MARCM clones of 1–5 cells without a neuroblast were also recovered in the late larval SEG; these cells may represent single cell MARCM clones, two cell MARCM clones or small multiple cell MARCM clones of postembryonic neurons that have lost their neuroblast due to termination of proliferation in early larval stages.)

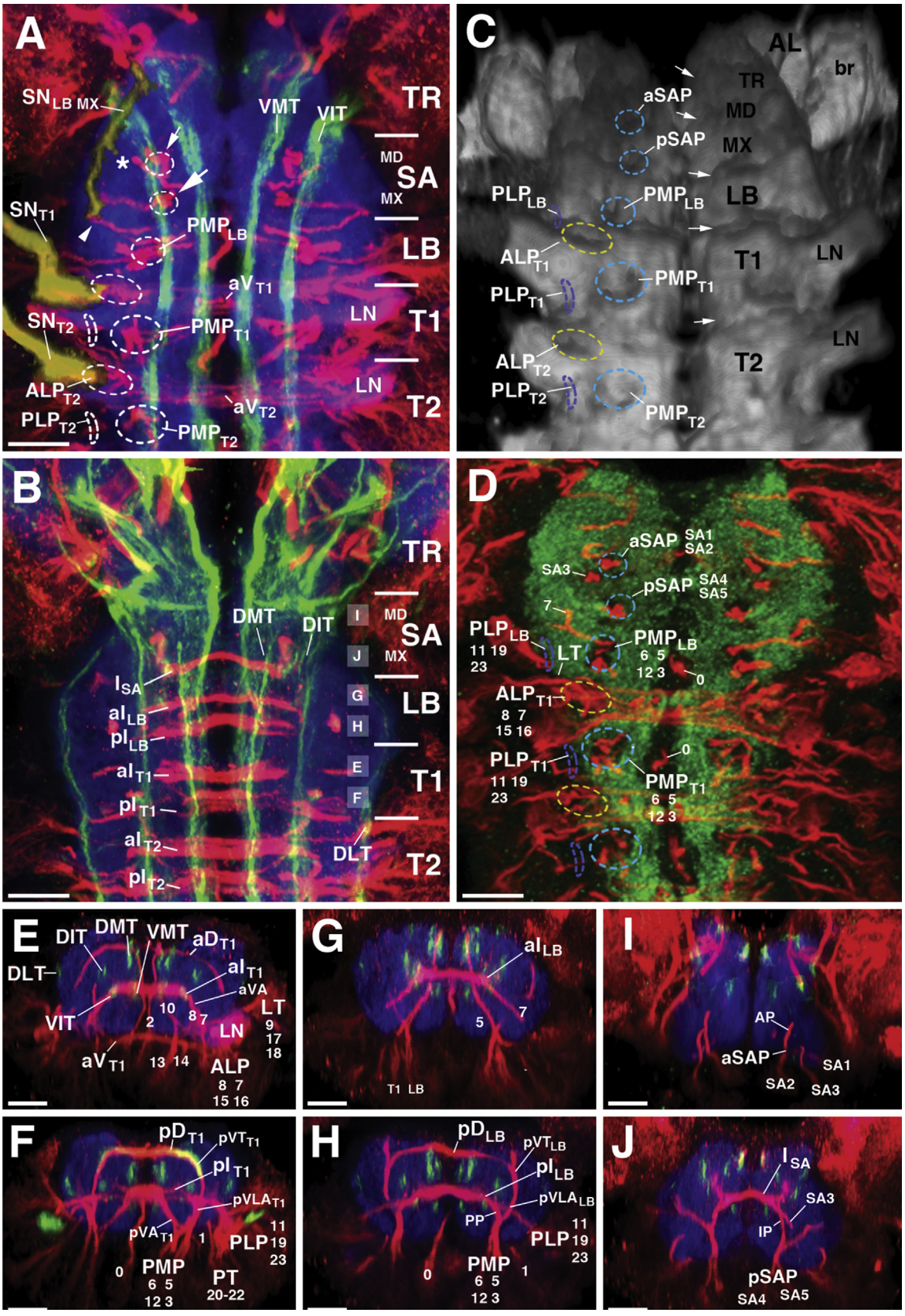

Complete MARCM-based identification of neuroblast lineages in the late larval SEG

Labial lineage 7 (*LB*7): Thoracic lineages 7 and 8 enter the neuropil together, project medially and cross in the anterior intermediate commissure. Lineage 8 also has an ipsilateral branch to the leg neuropil (Truman et al., 2004). In the SEG, one lineage resembles the 7/8 pair, projecting medially and forming a thin commissure (aI) anterior to the labial pI commissure (Fig. 2C). Since it has no additional ipsilateral branch we refer to it as labial lineage 7.

Labial lineage 5 (*LB*5): The single SAT of thoracic lineage 5 enters the neuropil lateral of 6 and projects medially following the 6c branch towards the pI commissure. Labial lineage 5 starts out at the same position as its thoracic counterparts, but does not cross the midline. Instead it projects dorsally between the labial pI and aI commissures, turns anteriorly, and extends along the dorsal surface of the SEG towards the SPG (Fig. 2D).

Labial lineage 3 (*LB*3): In thoracic segments, the lineage 3 SAT splits into two branches. One targets the leg neuropil, the second initially follows the tracts of lineages 6 and 12 dorsally in the posterior vertical tract (pVT). The labial lineage 3 does not follow 6 or 12; its thick SAT projects straight upward and, at the intersection of the posterior intermediate (pI_{LB}) commissure and dorsal intermediate tract (DIT), branches into a short medial component along the pI commissure and a longer anterior component extending along the DIT (Fig. 2E).

Labial lineage 6 (*LB*6): In the thoracic neuromeres, lineage 6 bifurcates and sends one branch (6 cm) through the pI commissure and another branch (6 cd) towards the dorsal neuropil. The labial lineage 6 SAT is less complex. Lacking most of the medial 6 cm branch, it continues vertically alongside lineage 12, then bends medially to form the pD commissure (Fig. 2F).

Labial lineage 12 (*LB*12): The SAT of lineage 12 in thoracic segments has an SAT which bifurcates into a medial branch (12c) and a lateral branch (12i) that splits into a longer dorsal branch (12id) following the posterior vertical tract and a shorter branch (12im) terminating in the neuropil flanking the DIT tract. Out of these three SAT branches, only one, 12id, is left in the labial lineage 12. It projects into the vertical tract and terminates in the dorsal neuropil (Dnp; Fig. 2G).

Labial lineage 0 (*LB*0): The cell body cluster of lineage 0 is located in the ventral midline (Fig. 1D). The unpaired SAT projects vertically and bifurcates at the level of the intermediate commissures. In the prothoracic neuromere, lineage 0 targets the posterior intermediate commissure; the labial lineage 0 projects further anteriorly to the anterior commissure (Fig. 2H).

Labial lineages 11, 19, 23 (*LB*11, *LB*19, *LB*23): The SATs of thoracic lineages 19 and 23 project medially in the neuropil and cross in the pI commissure. The SATs of labial lineages 19 and 23 are identical to their thoracic counterparts, crossing in the pI (Fig. 2I and J). Labial lineage 11 is located near the cell bodies of 19 and 23, but is rudimentary and has no obvious SAT pattern (Fig. S1).

SA lineages 1–5: Lineages SA2 and SA4 enter the anterior SEG neuropil together and end near to each other in the dorsal tract neuropil (Fig. 3D and F). Lineage SA1 lies laterally of SA2, projects medially, and terminates ventrally in the anterior SEG (Fig. 3C). SA3 enters the neuropil close to SA1 and SA2, but projects posteriorly and medially, and crosses the midline in the anterior-most commissure (I_{SA}; Fig. 3E). Finally, SA5 enters alongside SA4, then turns laterally to terminate in the dorsolateral neuropil (Fig. 3G).

Taken together, these MARCM experiments identify a small set of 14 neuroblast lineages (13 paired and 1 unpaired) that comprise adult-specific neurons in the SEG. The complete set of these identified neuroblast lineages as well as their spatial relationship to adjacent lineages in the prothoracic and tritocerebral neuromeres is shown in Fig. 4.

Reduction of neuroblast number during embryonic and larval development

Since both the analysis of identified SATs and the clonal MARCM experiments indicate that 14 neuroblast lineages comprise adult-specific neurons in the SEG during postembryonic development, most of the approximately 80 embryonic neuroblasts in the SEG (R. Urbach, personal communication) are likely to disappear during embryonic and/or larval development. To investigate this, we first determined the number of Deadpan-positive neuroblasts during embryogenesis from stage 12 onward. (The Hox gene *labial* was used to determine the anterior boundary of the developing SEG together with *engrailed* which marks the posterior boundaries of neuromeres.) A marked decline in the number of Deadpan-positive neuroblasts was indeed observed (Fig. 5A–C). Thus, while an average of 83 (s.d. $\pm$ 8, $n=10$) neuroblasts was seen in the SEG at embryonic stage 12, only an average of 24 (s.d. $\pm$ 5, $n=17$) neuroblasts were seen at embryonic stage 16.

These data are comparable to the reduction in neuroblast number reported for abdominal neuromeres, where the bulk of neuroblasts undergo apoptosis at the end of embryogenesis (White et al. 1994). To investigate if programmed cell death also underlies the reduction of neuroblast number in the embryonic SEG, we counted neuroblasts in the SEG of embryos that were homozygous for the apoptosis-inhibiting H99 allele (White et al., 1994). In contrast to the approximately 24 neuroblasts seen in stage 16 wildtype embryos, in H99 embryos 54 neuroblasts (s.d. $\pm$ 7, $n=8$) were observed in the SEG, suggesting that programmed cell death is involved in the reduction of neuroblast number seen in the late embryo (Fig. 5D).

To investigate if a further reduction in neuroblast number occurs during larval development of the SEG, we determined the number of Deadpan-positive neuroblasts in the SEG of L1–L3 larval stages (see again Fig. 5A). During early larval stages (L1 and L2), 19 neuroblasts (s.d. $\pm$ 1, $n=8$) were present in the SEG. In contrast, from the early L3 stage onward until the end of larval development only 14 neuroblasts were observed in the SEG. These data imply that a significant reduction in neuroblast number also occurs during postembryonic development; only 14 of the ca. 19 SEG neuroblasts seen in early larval stages remain present throughout larval development. This finding is in agreement with the results of the clonal MARCM experiments and the analysis of identifiable

Fig. 2. Secondary lineages of the posterior SEG (labial neuromere). (A and B): Transverse slices of subesophageal ganglion at the level of the anterior (A) and posterior (B) intermediate commissure of the labial neuromere (see panels G and H of Fig. 1 for details and abbreviations), illustrating position of the nine lineages of the posterior SEG (annotated by numbers) relative to commissures (aI_{LB}, pI_{LB}, pD_{LB}), connectives (FasII-positive, green), and entry portals (PMP, PLP). (C–J): *tubulin*-driven MARCM clones of individual SEG lineages induced at early larval stages. The lineage represented by a clone is identified alphanumerically at bottom right of top part of panel. Top parts of panels are z-projections of confocal sections oriented parallel to the length axis of the ventral nerve cord. BP106 labeling (red) shows intermediate level of neuropil (60–80 μm from ventral surface) containing commissures (I_{SA}, aI_{LB}, pI_{LB}). GFP-labeled clones (green) are shown as z-projections through entire dorsoventral diameter of nerve cord. Note spatial relationship of clone to pattern of BP106-labeled SATs, which is characteristic of each lineage. For the bottom part of each panel, confocal stacks were digitally rotated 90°, generating cross a sectional view of the labial neuromere corresponding to the slices shown in panels (A) and (B). Lineages LB7 (C) and LB5 (D) are located in the anterior part of labial neuromere; cross sectional views correspond to the level shown in panel (A). Note anterior intermediate commissure (aI_{LB}), formed by the SAT of lineage LB7. Arrowhead in (D) indicates conspicuous forward directed trajectory of lineage LB5. The remainder of the lineages, shown in panels (E–J), are located in the posterior part of the labial neuromere, corresponding to the level shown in panel (B). Note the posterior intermediate commissure (pI_{LB}), formed by lineages LB3, LB19, and LB23; posterior ventro-lateral arch ($pVLA_{LB}$) and posterior vertical tract (pVT_{LB}), formed by lineages LB6 and LB12, and posterior pillar (PP), formed by lineage LB3. Other abbreviations: DIT_{np} neuropil of dorso-intermediate tract. (A and B) posterior view; (C–J) ventral (upper) and posterior (lower) view. Scale bar: 30 μm in A and B; 20 μm in C–J.

SATs reported above, and supports the notion that a relatively small set of 14 neuroblasts give rise to the lineages of adult-specific SEG neurons throughout postembryonic development. Results presented below indicate that this reduction in neuroblast number during postembryonic development is due to Hox gene-dependent programmed cell death.

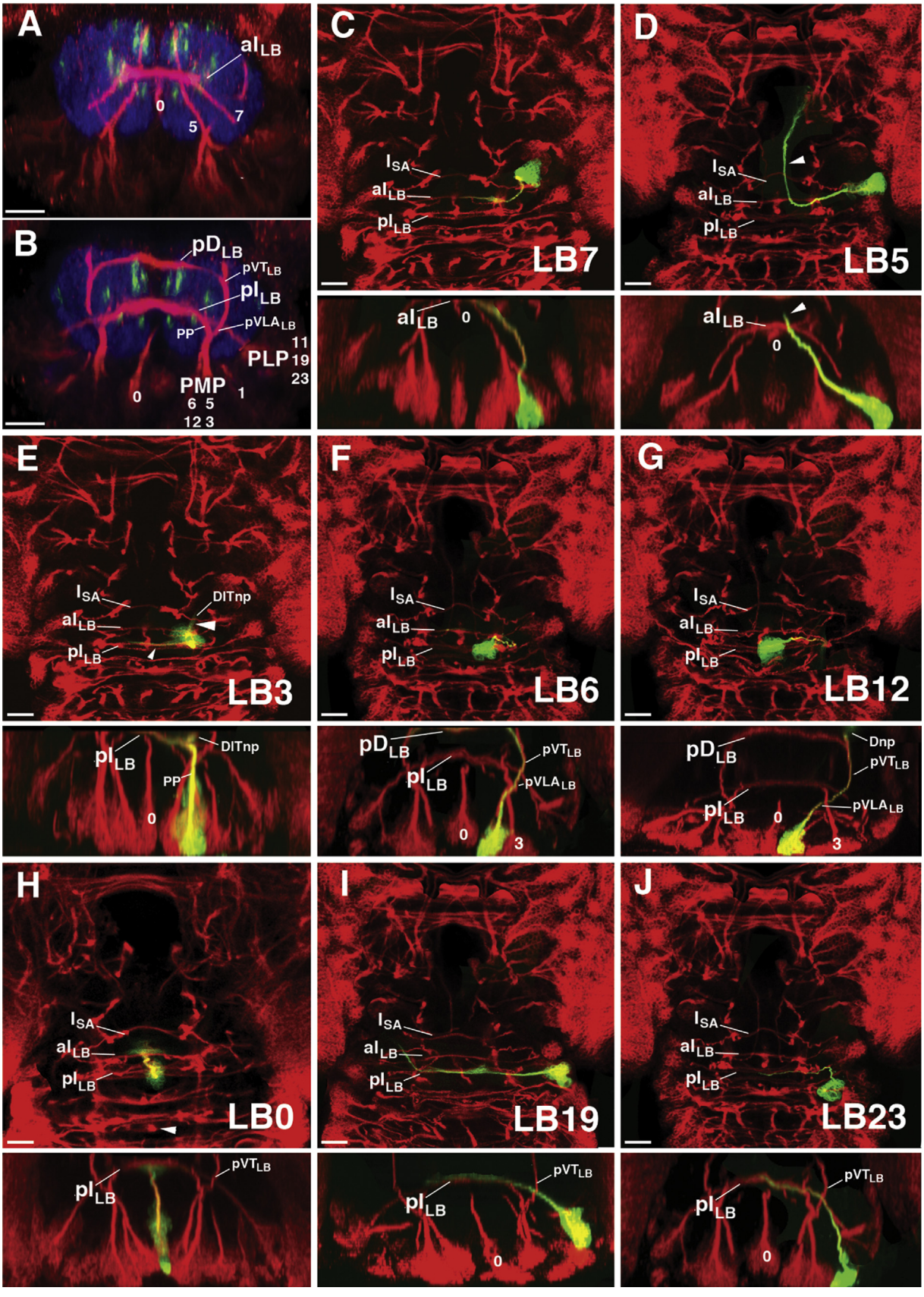

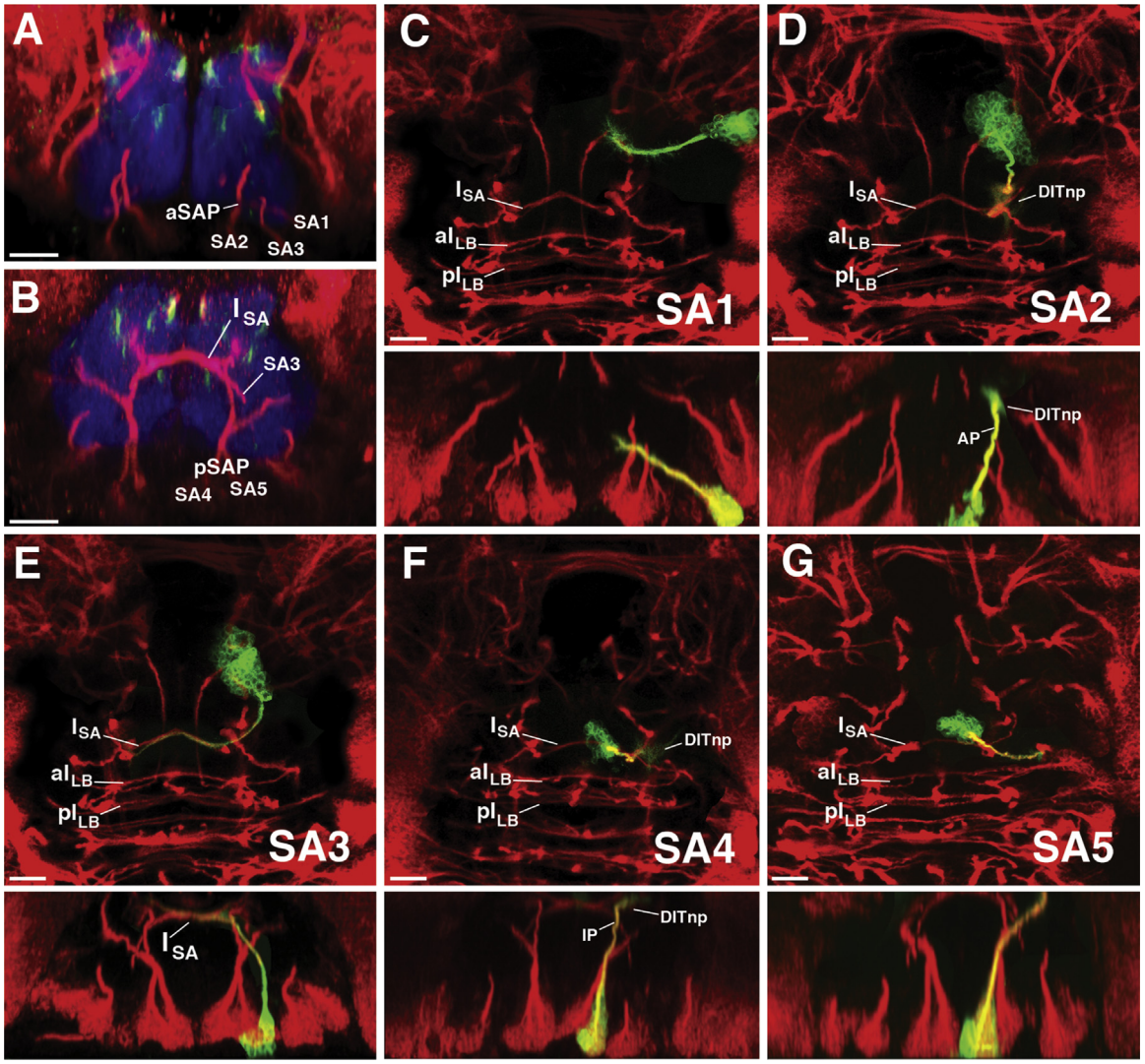

Fig. 3. Secondary lineages of the anterior SEG (SA domain). (A and B): Transverse slices of subesophageal ganglion at the level of the intermediate commissure of the anterior subesophageal ganglion (I_{SA}; panel B) and the level of the aSAP portal (A) (see panels I and J of Fig. 1 for details and abbreviations). (C–G): The five lineages of the anterior subesophageal ganglion (SA1-5) are illustrated in the same manner as described for labial lineages in Fig. 2. SA1 and SA2 (C and D) enter through the aSAP. SA1 terminates at a ventral level; SA2 projects dorsally, forming the anterior pillar (AP) and terminates at the level of the dorso-intermediate tract neuropil (DIT_{np}). SA3 (E) enters posteriorly adjacent to the aSAP, projects dorso-posteriorly and forms the I_{SA} commissure, the anterior-most BP106-positive commissure of the SEG. SA4 (F) and SA5 (G) enter through the pSAP. SA4 projects straight dorsally, forming the intermediate pillar of the anterior subesophageal ganglion (IP), and terminates in the DIT_{np}. SA5 follows SA4 in the intermediate pillar, but then veers off laterally to terminate in the dorso-lateral neuropil. (A and B) posterior view; (C–G) ventral (upper) and posterior (lower) view. Scale bar: 30 μm in A and B; 20 μm in C–G.

Lineage-specific expression of the Hox genes Dfd, Scr, and Antp in the larval SEG

During embryogenesis, the Hox genes *Deformed* (*Dfd*), *Sex combs reduced* (*Scr*), and *Antennapedia* (*Antp*) are expressed in an anteroposteriorly regionalized manner in the developing SEG (Hirth et al., 1998). To determine if these Hox genes are also expressed during postembryonic SEG development, we carried out an immunohistochemical analysis of late third instar larval brains. This analysis shows that *Dfd*, *Scr*, and *Antp* are indeed expressed postembryonically in broad, non-overlapping domains in the SEG (Fig. 6A–D).

To characterize the expression of these Hox genes in neuroblast lineages during postembryonic SEG development we combined MARCM labeling (for neuroanatomy see previous section) with co-immunolabeling for Dfd, Scr, and Antp. This analysis showed that most (11 out of 14) neuroblast lineages in the postembryonic SEG express one of the three Hox genes. *Dfd* is expressed in three lineages: SA1, SA2 (in both cases in most if not all cells, weakly in the NB), and SA3 (low albeit reproducible level; arrow) (Fig. 6E–G′). *Scr* is expressed in five lineages: SA4, SA5, LB5, LB6, and LB7 (in most cells, including the neuroblast; Fig. 6H–L′). *Antp* is expressed in three lineages: LB0, LB3, and LB19 (in a subset of cells, excluding the neuroblast; Fig. 6M–O′). The three remaining lineages, 11, 12, and 23, were not immunopositive for any of these Hox genes. In addition, 10 out of the 14 SEG lineages also express *engrailed* (Fig. S2) including all of the lineages that delimit the posterior boundary of the SEG. Hox gene and *engrailed* expression in the postembryonic SEG lineages are summarized in Fig. 6P.

Inactivation of Dfd, Scr, and Antp leads to axonal misprojections and neural cell number reduction in a subset of SEG lineages

To analyze the role of Hox genes in postembryonic SEG development, Dfd^{12} or Dfd^{16} mutant (42 specimens), Scr^{2} or Scr^{4} mutant (49 specimens) and $Antp^{25}$ or $Antp^{NS+RC3}$ mutant (24 specimens) MARCM clones were induced 24 h after larval hatching

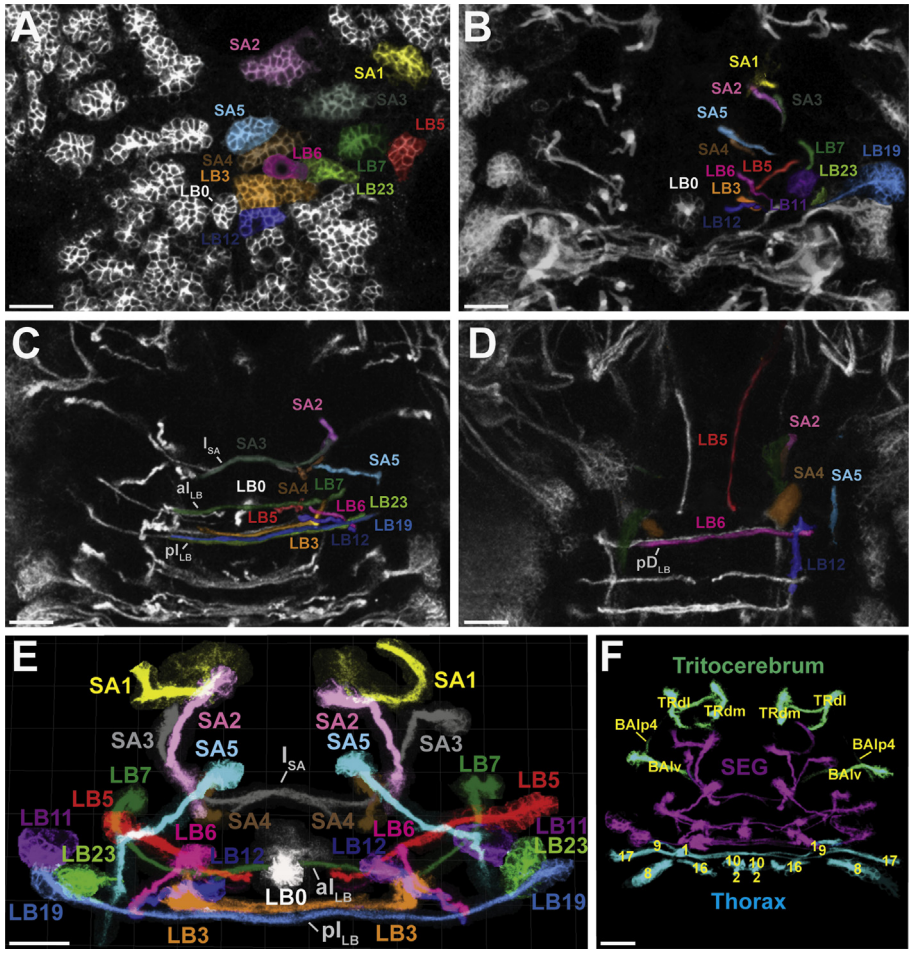

Fig. 4. Overview of the postembryonic SEG. (A–E) Color-coded overview (ventral view) of the 14 lineages in the postembryonic SEG as z-projections and as a 3D-reconstruction of their SATs. (A–D) represent different levels of focal planes of the same specimen. (F) 3D-reconstruction of secondary axon tracts of SEG and adjacent tritocerebral and thoracal lineages (same specimen as in Fig. 4E). Ventral view. Scale bars: 20 μm.

(ALH) and recovered in the late third larval stage. Hox gene loss-of-function resulted in axonal misprojections and/or cell number reduction in 4 out of 14 SEG lineages (Fig. 7A–H). (Mutant phenotypes were only seen in the lineages that normally express a given Hox gene, never in other lineages implying that non-cell autonomous effects of Hox mutations are absent.)

Clonal loss-of-function of *Dfd* resulted in a misprojection phenotype in SA1. In contrast to the medially projecting SAT of the wildtype lineage, the SAT of the *Dfd* mutant SA1 lineage projected posteriorly in the SEG (Fig. 7A and B; arrows). The same type of posterior misprojection phenotype was seen in most Dfd^{12} (8 out of 9) and all Dfd^{16} (5 out of 5) mutant SA1 clones indicating that the misprojection is not randomly directed in nature.

Clonal loss-of-function of *Scr* resulted in a misprojection phenotype in SA5 and a cell number reduction phenotype in LB5. Unlike the posteriorly projecting SAT of the wildtype SA5 lineage, the SAT of the *Scr* mutant SA5 lineage usually projected medially across the midline (Fig. 7C and D; arrows). Projection defects were observed in 10 out of 14 Scr^2 mutant clones and in 8 out of 10 Scr^4 mutant clones. The cell number in *Scr* mutant LB5 clones averaged 33 cells (s.d. ± 5 cells, $n=6$), in contrast to clones of the wildtype lineage LB5 which had an average of 61 cells (s.d. ± 3, $n=6$) (Fig. 7G). The *Scr* mutant SAT was, in consequence, considerably thinner in the wildtype, however, its projection pattern appeared normal. This reduction in cell number was not accompanied by loss of the LB5 neuroblast.

Clonal loss-of-function of *Antp* resulted in both a misprojection phenotype and a cell number reduction phenotype in LB3. Thus, while the wildtype LB3 SAT had an anterior as well as a medial branch, the *Antp* mutant SAT only retained the anterior branch (Fig. 7E and F; arrows). Furthermore, in contrast to wildtype LB3 lineages which averaged 129 cells (s.d. ± 5 cells, $n=5$), *Antp* mutant LB3 lineages had an average of 51 cells (s.d. ± 7 cells, $n=5$) (Fig. 7H). This reduction in cell number was also not associated with loss of the LB3 neuroblast.

The fact that the *Scr* mutant *LB5* and *Antp* mutant LB3 lineages contain about half of the cells present in the corresponding wildtype lineages, suggests that these Hox genes might be required to prevent hemilineage dependent programmed cell death (e.g. Kumar et al., 2009; Lin et al., 2010; Truman et al., 2010). In order to test this hypothesis, we examined the LB3 lineage in *Antp*-GFP preparations stained with antibodies for the Notch-activity reporter Hey (Monastirioti et al., 2010) and BP106 for lineage identification (data not shown). In these experiments we could not find evidence for hemilineage-specific expression of *Scr* or *Antp*. In the LB5 lineage, *Scr* is expressed in most cells but *Hey* only in 1–3 cells. In case of the LB3 lineage, many cells express only *Antp*, while fewer cells express only Hey or on the other hand, are double-positive or double-negative for *Antp* and *Hey*. Taken together, these data do not support a hemilineage-dependent mechanism for the role of *Scr* and *Antp* in inhibiting cell loss of the LB5 and LB3 lineages, respectively.

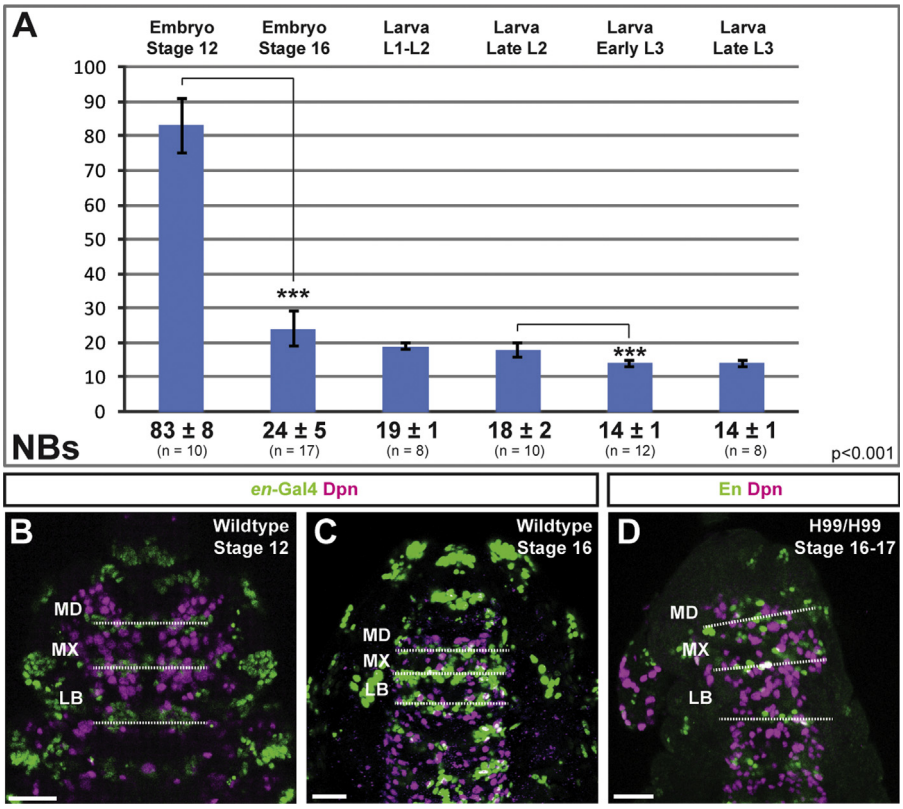

Fig. 5. Neuroblast numbers of the developing SEG. (A) Counts of Deadpan-positive neuroblasts in the developing SEG region, delimited by *labial* and *engrailed*. Between embryonic stage 12 and 16, the average neuroblast number in the SEG significantly decreases. Between late L2 and early L3 stages, another decrease in the average number of SEG neuroblasts is evident. $p < 0.001$. (B–D) Neuroblasts labeled by Dpn in the embryonic SEG. Neuromere borders are indicated by *engrailed*. MD, mandibular; MX, maxillary; LB, labium. (B) Wildtype stage 12 embryo, (C) wildtype stage 16 embryo, and (D) H99 homozygous stage 16–17 embryo. Ventral view. Scale bars: 20 μm.

In summary, Hox gene loss-of-function resulted in lineage-specific defects in a subset of those neuroblast lineages that are normally present in the SEG. A different type of Hox loss-of-function phenotype, which did not affect the normal SEG lineages, was also observed. This phenotype was the appearance of ectopic lineages that are never seen in the wildtype SEG.

Clonal loss-of-function of Dfd and Scr leads to ectopic lineage formation in the SEG

Among the randomly induced *Dfd* and *Scr* mutant MARCM clones, we consistently found five ectopic neuroblast lineage types that were never recovered in the wildtype brain (Fig. 7I–M). Since these ectopic neuroblast clone types could be identified based on their anatomical features, we refer to them as the Ect1^{Dfd}, Ect2^{Dfd}, Ect1^{Scr}, Ect2^{Scr}, and Ect3^{Scr} lineages. The Ect1^{Dfd} lineage was located posterior to the SA2 and SA3 lineages and projected its SAT antero-medially (Fig. 7I). The Ect2^{Dfd} lineage was located lateral to SA3 and projected medially (Fig. 7J). Quantification of cell body number showed that the Ect1^{Dfd} lineage had an average of 67 cells (s.d. ± 4, $n=10$) and Ect2^{Dfd} had an average of 37 cells (s.d. ± 1, $n=2$). Ect1^{Scr} was located adjacent to the SA4 and SA5 lineages, projected its SAT medially and contained an average number of 47 cells (s.d. ± 5 cells, $n=5$; Fig. 7K). The other ectopic lineages, termed Ect2^{Scr} and Ect3^{Scr}, were located more lateral to the SA4 and SA5 lineages, projected their SATs medially (Fig. 7L–M). They comprised an average number of 53 (Ect2^{Scr}; s.d. ± 4 cells, $n=4$) and 62 cells (Ect3^{Scr}; s.d. ± 5 cells, $n=4$).

Taken together this mutant analysis indicates that *Dfd* and *Scr* are required to prevent the formation of five ectopic neuroblast lineages in the wildtype. (Unlike *Dfd* and *Scr*, *Antp* does not appear to be required to prevent the formation of ectopic lineages in the SEG.) Based on previous findings in the abdominal and tritocerebral neuromeres (Bello et al., 2003; Kuert et al., 2012), it seems likely that the Hox genes *Dfd* and *Scr* might prevent the formation of ectopic neuroblast lineages in the wildtype larval SEG by inducing apoptosis of the corresponding neuroblasts. To investigate this, we performed a clonal MARCM analysis using the H99 allele (White et al., 1994). Apoptosis blocked MARCM neuroblast clones were induced at 24 hours ALH, recovered in late third larval stage brains, and co-labeled with anti-Dfd or anti-Scr antibodies ($n=184$ specimens). In these experiments, we consistently recovered two ectopic neuroblast lineage types that expressed *Dfd* and three types that expressed *Scr*.

The first *Dfd* expressing ectopic lineage, Ect1$^{Dfd\mathbf{H99}}$, was located posterior to the SA1 and SA2 lineage, projected its SAT bundle anteriorly, and had an average number of 71 cells (s.d. ± 14 cells, $n=4$; Fig. 8A and A′). The Ect2$^{Dfd\mathbf{H99}}$, was positioned lateral to the SA3 lineage, projected its SAT in a medial and anterior branch, and had an average number of 46 cells (s.d. ± 13 cells, $n=5$; Fig. 8B and B′). The *Scr* expressing ectopic lineage Ect1$^{Scr\mathbf{H99}}$ was located posterior to the SA4 and SA5 lineages, had a SAT that splits into a medial and a lateral branch, and had an average number of 83 cells (s.d. ± 9 cells, $n=5$; Fig. 8C and C′). The other two *Scr*-expressing lineages were located lateral to the SA5 and SA4 lineages, projected their SATs medially, and had an average cell number of 47 cells (s.d. ± 9 cells, $n=5$) (Fig. 8D and D′). Since these two lineages could be recovered together but not distinguished on a neuroanatomical basis, we refer to these ectopic lineages as Ect2/3$^{Scr\mathbf{H99}}$.

The Hox expressing ectopic lineages found in the apoptosis-blocked MARCM assay were remarkably similar in neuroanatomical respects to those found in the corresponding *Dfd* or *Scr* mutant MARCM experiments. (Differences between cell numbers of Hox

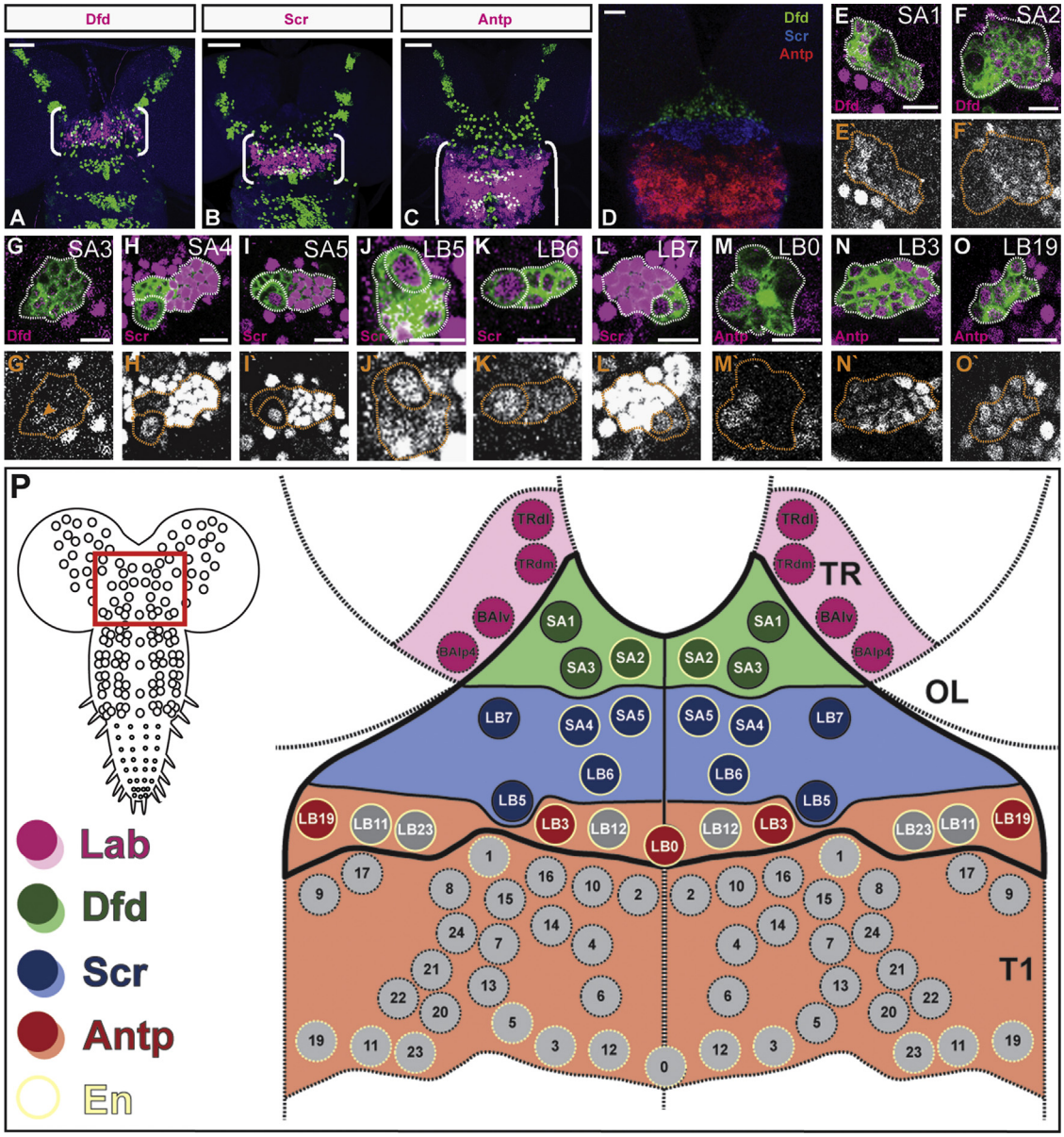

Fig. 6. Hox gene expression in the postembryonic SEG. (A–C) Immunolabeling of Hox proteins in late L3 brains co-expressing *engrailed*-Gal4 driven GFP. Z-projections of multiple optical sections. (D) Immunolabeling of antibodies against Dfd, Scr and Antp in a late L3 brain. Single section. (E–O′) MARCM clones of postembryonic SEG lineages, immunostained for Dfd (E–G′), Scr (H–L′) and Antp (M–O′). Single optical sections. (P) Summary scheme of Hox and *engrailed* expression in the postembryonic SEG. Lineages are represented as color-coded circles. Hatched circles indicate tritocerebral (TR) and thoracal (T1) lineages. Ventral view. Scale bars: 30 μm in A–C; 20 μm in D; and 10 μm in E–O.

gene mutant and apoptosis-blocked ectopic lineages may arise from Hox gene independent cell death of postmitotic cells.) These findings imply that the Hox genes *Dfd* and *Scr* are required in these five (ectopic) neuroblast lineages for termination of proliferation through programmed cell death during early postembryonic SEG development.

Discussion

In this report, we focus on the postembryonic neuroblast lineages that give rise to the adult-specific neurons of the SEG. We report three main findings. First, a small set of 14 uniquely identifiable postembryonic neuroblast lineages gives rise to secondary neurons in the postembryonic SEG. Second, the Hox genes *Dfd*, *Scr*, and *Antp* are expressed in a lineage-specific manner in the developing larval SEG. Third, loss-of-function analyses reveal lineage-specific requirements of these Hox genes in SEG development. In the following, we will discuss the major implications of these findings.

Reduced number of proliferating neuroblast lineages in postembryonic SEG development

A total of 14 identified postembryonic neuroblast lineages generate the adult-specific secondary neurons in the larval SEG. This is a surprisingly small number compared with the approximately 80 neuroblast lineages in the embryonic SEG (R. Urbach, personal communication). Our cell counts indicate that only about one fourth of these ca. 80 neuroblasts are reactivated postembryonically. This is markedly different in the SPG, where about 85 of the 100 embryonically active neuroblasts are reactivated and proliferate in larval stages (Dumstrei et al., 2003; Ito and Hotta, 1992; Pereanu and Hartenstein, 2006). Our experiments indicate

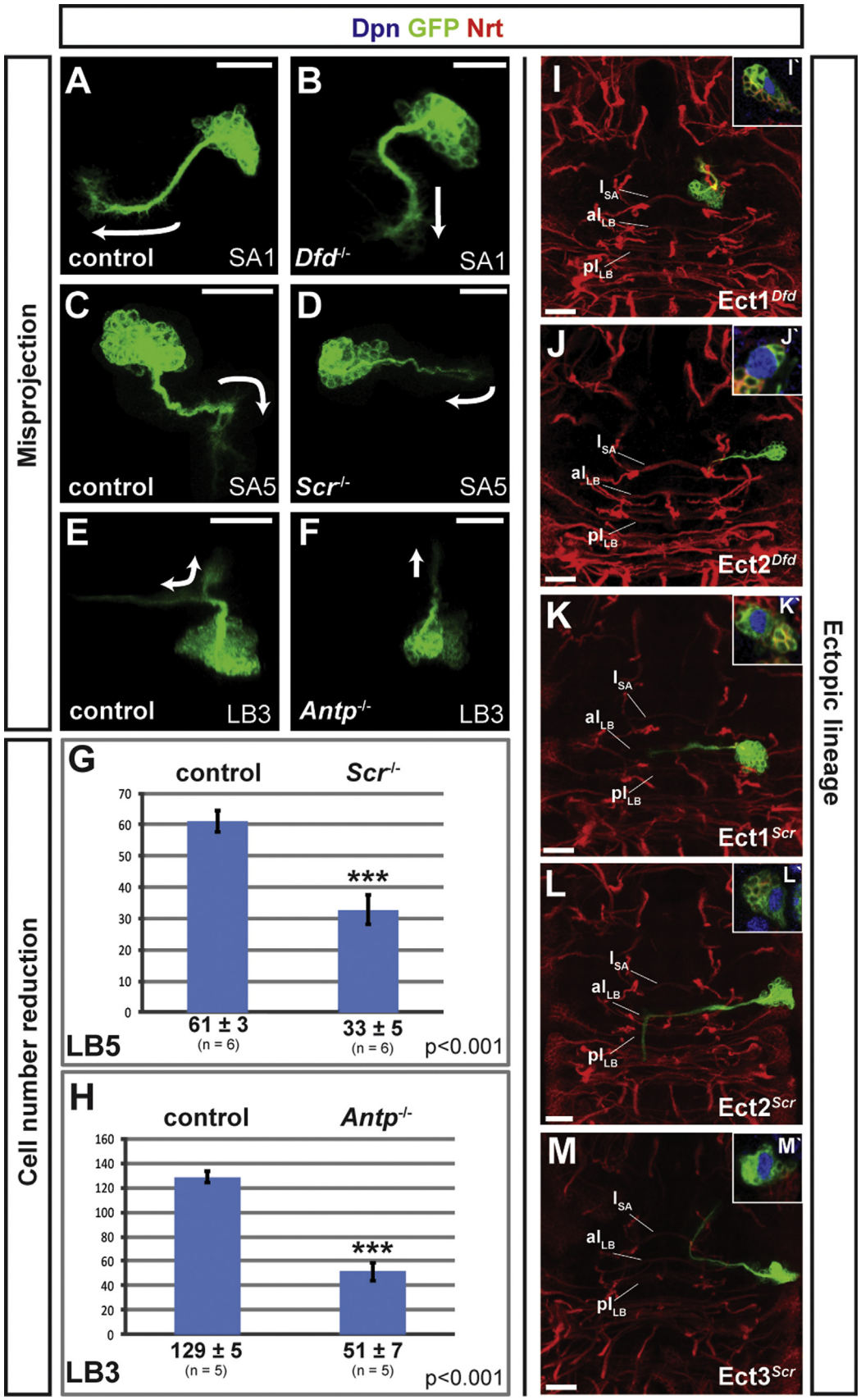

Fig. 7. Phenotypes of Hox gene inactivation in the postembryonic SEG. MARCM clones (GFP) in L3 brains, immunostained with anti-BP106 (Nrt) and Deadpan (Dpn). (A–F) Misprojection phenotypes in Hox mutant lineages. (A) Wildtype SA1 projects SAT medially (B) *Dfd*^{16} mutant SA1 misprojects SAT posteriorly. (C) Wildtype SA5 projects SAT laterally and subsequently posteriorly. (D) *Scr*^{2} mutant SA5 misprojects SAT medially. (E) Wildtype lineage LB3 has SAT that splits into anterior and medial branches. (F) *Antp*^{25} mutant clone of lineage LB3 retains only anterior SAT branch. (G–H) Cell number reduction phenotypes of Hox mutant lineages. (G) The average cell number of LB5 in wildtype and *Scr* mutant clones are significantly different. $p < 0.001$. (H) Average cell number of lineage LB3 in wildtype and *Antp*^{25} mutant clones are significantly different. $p < 0.001$. (I–M) Ectopic lineage formation induced by Hox mutation. (I) Ect1^{Dfd} with anterior-medial SAT projection. (J) Ect2^{Dfd} with medial SAT projection, (K) Ect1^{Scr} with medial SAT projection. (L) Ect2^{Scr} projects SAT medially. (M) Ect3^{Scr} with medial-anterior SAT projection. Ventral view. Scale bars: 20 μm.

that the fate of half of the embryonic SEG neuroblasts that are not present postembryonically is programmed cell death. This situation is comparable to that of embryonic neuroblasts in the abdominal ganglia where the majority of neuroblasts undergo apoptosis at the end of embryogenesis (White et al., 1994; Peterson et al., 2002; Technau et al., 2006). The molecular cues which trigger cell death in these embryonic neuroblasts have not been studied. The fate of the other half of the embryonic SEG neuroblasts is unknown. They may terminate proliferation through other *reaper*/*hid*/*grim*-independent cell death mechanisms or through cell cycle exit at the end of embryogenesis. Further experiments will be necessary to elucidate this.

The low number of postembryonic SEG lineages has interesting consequences for the relationship between primary neurons and secondary neurons in the mature SEG. Most neuroblasts generate 10–20 neural cells embryonically and 100–150 neural cells postembryonically (see Hartenstein et al., 2008; Technau et al., 2006). Thus, the ca. 80 embryonic SEG neuroblasts should generate 800–1600 primary neural cells per hemiganglion while the 14 postembryonic neuroblasts generate approximately 900 secondary neural cells (as estimated by our cell counts) per hemiganglion. Assuming that most of the primary neurons survive metamorphosis, this suggests that a substantial fraction of the neurons in the adult SEG could be primary neurons that comprise the functional larval SEG before their integration into the adult brain.

Previous work has shown that 75 neuroblast lineages generate the secondary neurons of the three thoracic neuromeres (Ito and Hotta, 1992; Marin et al., 2012; Truman et al., 2004). This is in striking contrast to the 14 neuroblast lineages that generate secondary neurons in the three SEG neuromeres. This reduction is most evident in the SA region, where only one commissure (I_{SA}) is present which is also formed by only one lineage, SA3. The labial neuromere is also reduced but not as dramatically. Moreover, it retains the two commissures (aI, pI) which are also characteristic of the thoracic neuromeres. This relatively small number of postembryonic neuroblast lineages in the SEG neuromeres is likely to reflect the marked reduction and fusion of segmental appendages in the three gnathal segments that are innervated by the SEG. From an evolutionary perspective, a loss/reduction of gnathal appendages in insects such as flies would eliminate or reduce the need for corresponding neural control circuitry at least in the adult. Interestingly, and in contrast to the VNC, we found no evidence for the presence of postembryonically generated motoneurons in the SEG, indicating that all secondary neurons in the SEG are interneurons. This notion is supported by the fact that none of the 14 SEG neuroblast lineages join the labial or pharyngeal nerves (which contain the motor axons from the proboscis), but instead they project their SATs to areas within the CNS.

Regionalized expression of Hox genes in postembryonic SEG development

During embryonic and postembryonic brain development, the Hox genes *Dfd*, *Scr*, and *Antp* are regionally expressed in discrete and largely non-overlapping domains in the neuromeres of the SEG (Hirth et al., 1998; this report). In both cases *Dfd* is expressed

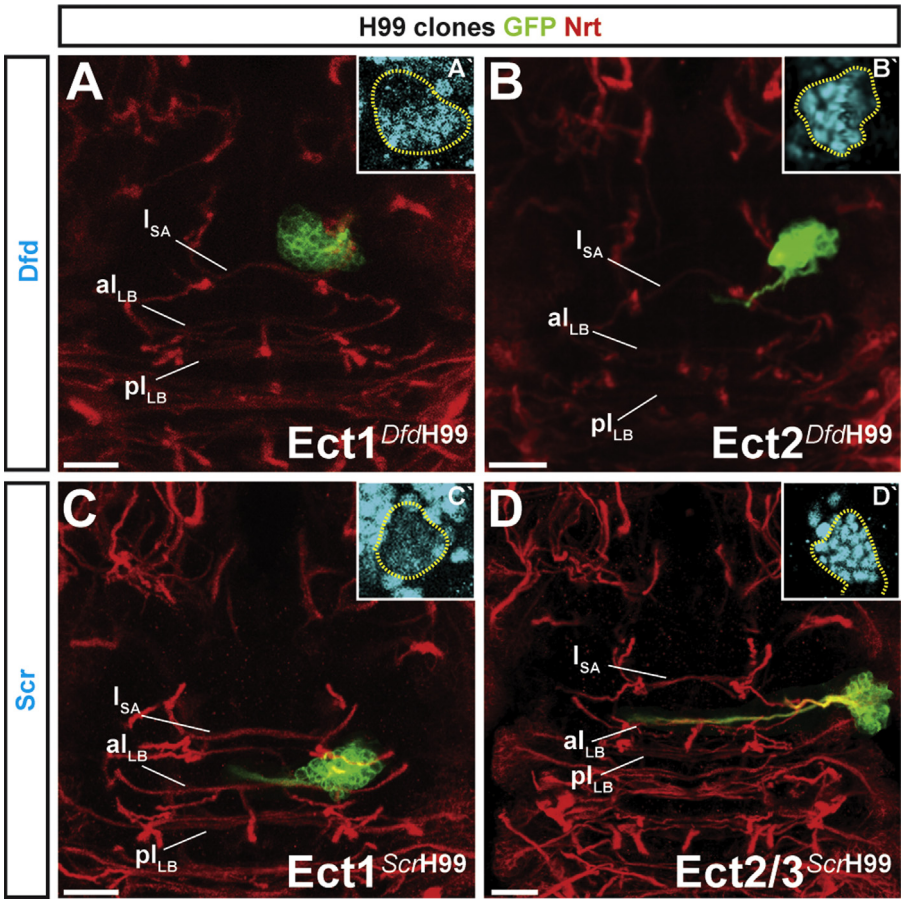

Fig. 8. Clonal cell death block induces Hox expressing ectopic lineages. MARCM clones homozygous for H99 (GFP), in L3 brains immunostained with anti-BP106 (Nrt). (A) Ect1$^{Dfd\mathbf{H99}}$ projects short SAT branch anteriorly. (A′) Expression of *Dfd* in Ect1$^{Dfd\mathbf{H99}}$. (B) Ect2$^{Dfd\mathbf{H99}}$ projects its SAT in medial direction. (B′) Expression of *Dfd* in Ect2$^{Dfd\mathbf{H99}}$. (C) Ect1$^{Scr\mathbf{H99}}$ located posterior to SA4 and SA5 projects SAT in a bifurcating bundle. (C′) Expression of *Scr* in Ect1$^{Scr\mathbf{H99}}$. (D) Ect2/3$^{Scr\mathbf{H99}}$ projects SAT medially. (D′) Expression of *Scr* in Ect2/3$^{Scr\mathbf{H99}}$. Ventral view. Scale bars: 20 μm.

in an anterior domain, *Scr* is expressed in a posteriorly adjacent domain, and *Antp* expression begins in a small labial domain adjacent to the prothoracic neuromere. Moreover, while the total number of neuroblast lineages that express a given Hox gene may be different embryonically and postembryonically, most of the postembryonic neuroblast lineages do express one of these genes suggesting that Hox gene expression is a stable developmental feature of SEG lineages. Indeed, most if not all of the Hox genes that are expressed in the embryonic CNS, are re-expressed in the neuroblast lineages of the postembryonic CNS (Bello et al., 2003; Hirth et al., 1998; Kuert et al., 2012; Marin et al., 2012; this report).

Hox genes are known to be expressed during CNS development in a number of bilaterian animal groups, including vertebrates, hemichordates, insects, and annelids, and in all of these animal groups the order of Hox gene expression domains in the developing CNS appears to be conserved (see Reichert and Bello, 2010). For example, the order of expression of orthologous Hox genes in the developing CNS of *Drosophila*, mouse, and human is virtually identical (Hirth et al., 1998; Graham et al., 1989; Wilkinson et al., 1989; Hunt and Krumlauf, 1991; Vieille-Grosjean et al., 1997). Taken together, these findings suggest that a conserved pattern of Hox gene expression domains may be a common feature in the developing CNS of all bilaterians.

Two types of lineage-specific function of Hox genes in postembryonic SEG development

Our study reveals two types of lineage-specific requirement for Hox genes during postembryonic SEG development. The first is a requirement of the Hox genes *Dfd*, *Scr* and *Antp* for correct postembryonic development of a subset of those lineages that are normally present in the wildtype SEG. Hox genes are required for correct SAT projections in the lineages SA1 (*Dfd*), SA5 (*Scr*) and LB3 (*Antp*). Interestingly, in all three cases the lineage-specific loss-of-function of these Hox genes results in specific, reproducible SAT misprojections and not in randomized axonal misprojections. While this could, in principle, be the result of a homeotic transformation phenotype, we find no evidence for such a transformation, since in terms of their projection patterns mutant SATs of these three lineages do not resemble any of the wildtype SATs present in the larval SEG.

Hox genes are also required for correct cell number in the lineages LB5 (*Scr*) and LB3 (*Antp*). While these Hox mutant lineages lose about half of their cells, which would suggest the involvement cell death in a hemilineage-dependent manner, we could not find evidence for hemilineage-specific Hox gene expression in these lineages. Thus, further studies of Hox gene action in the lineages LB3 and LB5 are necessary to dissect the functional requirement of *Scr* and *Antp* in lineage-specific cell survival.

The second type of lineage-specific requirement for Hox genes during postembryonic SEG development is the prevention of ectopic lineage formation. Thus, in addition to their requirement for correct development of normal wildtype lineages, the genes *Dfd* and *Scr* are also required for suppressing the appearance of aberrant ectopic lineages that are not normally present in the wildtype SEG. When *Dfd* or *Scr* mutant neuroblast clones are induced at early larval stages and recovered at late larval stages, five distinct types of ectopic neuroblast clones are found. Each of these is identifiable based on reproducible neuroanatomical features such as position, secondary axon tract projection and cell number. These ectopic lineages do not represent homeotic transformations of other wildtype neuroblast lineages, since all other SEG neuroblast lineages are present. Whether these ectopic lineages become functionally integrated into the adult brain of *Drosophila* is currently unknown. Evidence for an integration of ectopic neuron groups into a mature brain comes from mammalian studies, which show that *Hoxa1* mutant hindbrain progenitors can establish supernumerary ectopic neural cell groups that escape apoptosis and give rise to a functional circuit in the postnatal brain (del Toro et al., 2001).

The molecular regulators through which the Hox genes *Dfd*, *Scr* and *Antp* exert their diverse roles in lineage-specific SEG development are currently not known. In terms of the Hox gene requirement for correct development of wildtype lineages, only 4 of the 14 SEG lineages (11 of which express Hox genes) show misprojection or cell number mutant phenotypes. However, in these 4 lineages, the Hox gene mutant phenotypes are highly penetrant and reproducible. The lineage-restricted nature of these mutant phenotypes suggests that Hox genes interact with other lineally acting control elements to determine the developmental features of the affected lineages. While the ensemble of these control elements is currently unknown, there is increasing evidence for the importance of transcription factor codes in controlling the expression of axonal guidance molecules (see Butler and Tear, 2007; Guthrie, 2007). In terms of the Hox gene requirement for preventing the formation of ectopic lineages, our data suggest that this involves lineage-specific programmed cell death of the corresponding postembryonic neuroblasts. Indeed, all Hox genes studied to date have been implicated in some aspect of programmed cell death in postembryonic neuroblasts. The *lab* gene is required for the termination of specific tritocerebral neuroblasts, *Dfd* and *Scr* are required for lineage-specific neuroblast termination in the SEG, *Antp* und *Ubx* can trigger neuroblast death if misexpressed in thoracic lineages, and *abd-A* induces programmed cell death in neuroblasts of the central abdomen (Bello et al., 2003; Kuert et al., 2012; Marin et al., 2012). We therefore conclude that a general function of Hox genes in postembryonic neural development is in the regionalized termination of progenitor proliferation as a key mechanism for neuromere-specific differentiation and specialization of the adult brain.

Acknowledgments

We thank Rolf Urbach, Amelia Younossi-Hartenstein and Susanne Flister. Supported by the Swiss NSF and the Sinergia Program CRSII3 136307.

Appendix A. Supporting information

Supplementary data associated with this article can be found in the online version at http://dx.doi.org/10.1016/j.ydbio.2014.03.021.

References

Bello, B.C., Hirth, F., Gould, A.P., 2003. A pulse of the *Drosophila* Hox protein abdominal-A schedules the end of neural proliferation via neuroblast apoptosis. Neuron 37, 209–219.

Bello, B.C., Holbro, N., Reichert, H., 2007. Polycomb group genes are required for neural stem cell survival in postembryonic neurogenesis of *Drosophila*. Development 134, 1091–1099.

Bossing, T., Udolph, G., Doe, C.Q., Technau, G.M., 1996. The embryonic central nervous system lineages of *Drosophila melanogaster*. I. Neuroblast lineages derived from the ventral half of the neuroectoderm. Dev. Biol. 179, 41–64.

Brierley, D.J., Rathore, K., VijayRaghavan, K., Williams, D.W., 2012. Developmental origins and architecture of *Drosophila* leg motoneurons. J. Comp. Neurol. 520, 1629–1649.

Butler, S.J., Tear, G., 2007. Getting axons into the right path: the role of transcription factors in axon guidance. Development 134, 439–448.

Cardona, A., Larsen, C., Hartenstein, V., 2009. Neuronal fiber tracts connecting the brain and ventral nerve cord of the early *Drosophila* larva. J. Comp. Neurol. 515, 427–440.

Condie, J.M., Mustard, J.A., Brower, D.L., 1991. Generation of anti-*Antennapedia* monoclonal antibodies and *Antennapedia* protein expression in imaginal discs. Drosoph. Inf. Serv. 70, 52–54.

Del Toro, E.D., Borday, V., Davenne, M., Neun, R., Rijli, F.M., Champagnat, J., 2001. Generation of a novel functional neuronal circuit in *Hoxa1* mutant mice. J. Neurosci. 21, 5637–5642.
Doe, C.Q., 1992. Molecular markers for identified neuroblasts and ganglion mother cells in the *Drosophila* central nervous system. Development 116, 855–863.
Dumstrei, K., Wang, F., Nassif, C., Hartenstein, V., 2003. Early development of the *Drosophila* brain: V. Pattern of postembryonic neuronal lineages expressing DE-cadherin. J. Comp. Neurol. 455, 451–462.
Egger, B., Chell, J.M., Brand, A.H., 2008. Insights into neural stem cell biology from flies. Philos. Trans. R. Soc. Lond. B: Biol. Sci. 363, 39–56.
Graham, A., Papalopulu, N., Krumlauf, R., 1989. The murine and *Drosophila* homeobox gene complexes have common features of organization and expression. Cell 57, 367–378.
Guthrie, S., 2007. Patterning and axon guidance of cranial motor neurons. Nat. Rev. Neurosci. 8, 859–871.
Hartenstein, V., Spindler, S., Pereanu, W., Fung, S., 2008. The development of the *Drosophila* larval brain. Adv. Exp. Med. Biol. 628, 1–31.
Hirth, F., Hartmann, B., Reichert, H., 1998. Homeotic gene action in embryonic brain development of *Drosophila*. Development 125, 1579–1589.
Hunt, P., Krumlauf, R., 1991. Deciphering the Hox code: clues to patterning branchial regions of the head. Cell 66, 1075–1078.
Ito, K., Hotta, Y., 1992. Proliferation pattern of postembryonic neuroblasts in the brain of *Drosophila melanogaster*. Dev. Biol. 149, 134–148.
Ito, M., Masuda, N., Shinomiya, K., Endo, K., Ito, K., 2013. Systemic analysis of neural projections reveals clonal composition of the *Drosophila* brain. Curr. Biol. 23, 644–655.
Kuert, P.A., Bello, B.C., Reichert, H., 2012. The *labial* gene is required to terminate proliferation of identified neuroblasts in postembryonic development of the *Drosophila* brain. Biol. Open 1, 1016–1023.
Kumar, A., Bello, B., Reichert, H., 2009. Lineage-specific cell death in postembryonic brain development of *Drosophila*. Development 130, 3433–3442.
Landgraf, M., Sanchez-Soriano, N., Technau, G.M., Urban, J., Prokop, A., 2003. Charting the *Drosophila* neuropile: a strategy for the standardised characterisation of genetically amenable neurites. Dev. Biol. 260, 207–225.
Lee, T., Luo, L., 1999. Mosaic analysis with a repressible cell marker for studies of gene function in neuronal morphogenesis. Neuron 22, 451–461.
Lee, T., Luo, L., 2001. Mosaic analysis with a repressible cell marker (MARCM) for *Drosophila* neural development. Trends Neurosci. 24, 251–254.
LeMotte, P.K., Kuroiwa, A., Fessler, L.I., Gehring, W.J., 1989. The homeotic gene *Sex Combs Reduced* of *Drosophila*: gene structure and embryonic expression. EMBO J. 8, 219–227.
Lin, S., Lai, S.L., Yu, H.H., Chihara, T., Luo, L., Lee, T., 2010. Lineage-specific effects of Notch/Numb signaling in post-embryonic development of the *Drosophila* brain. Development 137, 43–51.
Lovick, J.K., Omoto, J.J., Wong, D.C., Nguyen, J.D., Hartenstein, V., 2013. Postembryonic lineages of the Drosophila brain: I. Development of the lineage-associated fiber tracts. Dev. Biol. 384, 228–257.
Marin, E.C., Dry, K.E., Alaimo, D.R., Rudd, K.T., Cillo, A.R., Clenshaw, M.E., Negre, N., White, K.P., Truman, J.W., 2012. *Ultrabithorax* confers spatial identity in a context-specific manner in the *Drosophila* postembryonic ventral nervous system. Neural Dev. 7, 31.
Monastirioti, M., Giagtzoglou, N., Koumbanakis, K.A., Zacharioudaki, E., Deligiannaki, M., Wech, I., Almeida, M., Preiss, A., Bray, S., Delidakis, C., 2010. *Drosophila* Hey is a target of Notch in asymmetric divisions during embryonic and larval neurogenesis. Development 137, 191–201.
Nassif, C., Noveen, A., Hartenstein, V., 2003. Early development of the *Drosophila* brain: III. The pattern of neuropile founder tracts during the larval period. J. Comp. Neurol. 455, 417–434.
Patel, N., 1994. Imaging neuronal subsets and other cell types in whole mount *Drosophila melanogaster* embryos and larvae using antibody probes. In: Goldstein, L.S.B., Fyrberg, E.A. (Eds.), *Drosophila melanogaster*: Practical Uses in Cell and Molecular Biology. Academic Press, New York.
Percival-Smith, A., Weber, J., Gilfoyle, E., Wilson, P., 1997. Genetic characterization of the role of the two HOX proteins, Proboscipedia and Sex Combs Reduced, in determination of adult antennal, tarsal, maxillary palp and proboscis identities in *Drosophila melanogaster*. Development 124, 5049–5062.
Pereanu, W., Hartenstein, V., 2006. Neural lineages of the *Drosophila* brain: a three-dimensional digital atlas of the pattern of lineage location and projection at the late larval stage. J. Neurosci. 26, 5534–5553.
Peterson, C., Carney, G.E., Taylor, B.J., White, K., 2002. Reaper is required for neuroblast apoptosis during *Drosophila* development. Development 129, 1467–1476.
Pflüger, H.J., Braeunig, P., Hustert, R., 1988. The organization of mechanosensory neuropiles in locust thoracic ganglia. Philos. Trans. R. Soc. Lond. B 321, 1–26.
Power, M.E., 1948. The thoraco-abdominal nervous system of an adult insect *Drosophila melanogaster*. J. Comp. Neurol. 88, 347–409.
Schmid, A., Chiba, A., Doe, C.Q., 1999. Clonal analysis of *Drosophila* embryonic neuroblasts: neural cell types, axon projections and muscle targets. Development 126, 4653–4689.
Schmidt, H., Rickert, C., Bossing, T., Vef, O., Urban, J., Technau, G.M., 1997. The embryonic central nervous system lineages of *Drosophila melanogaster*. II. Neuroblast lineages derived from the dorsal part of the neuroectoderm. Dev. Biol. 189, 186–204.
Siebert, M., Banovic, D., Goellner, B., Aberle, H., 2009. *Drosophila* motor axons recognize and follow a sidestep-labeled substrate pathway to reach their target fields. Genes Dev. 2, 1052–1062.
Technau, G.M., Berger, C., Urbach, R., 2006. Generation of cell diversity and segmental pattern in the embryonic central nervous system of *Drosophila*. Dev. Dyn. 235, 861–869.
Truman, J.W., Schuppe, H., Shepherd, D., Williams, D.W., 2004. Developmental architecture of adult-specific lineages in the ventral CNS of *Drosophila*. Development 131, 5167–5184.
Truman, J.W., Moats, W., Altman, J., Marin, E.C., Williams, D.W., 2010. Role of Notch signaling in establishing the hemilineages of secondary neurons in *Drosophila melanogaster*. Development 137, 53–61.
Tyrer, N.M., Gregory, G.E., 1982. A guide to the neuroanatomy of locust suboesophageal and thoracic ganglia. Philos. Trans. R. Soc. Lond. B 297, 91–123.
Urbach, R., Technau, G.M., 2003. Molecular markers for identified neuroblasts in the developing brain of *Drosophila*. Development 130, 3621–3637.
Urbach, R., Technau, G.M., 2004. Neuroblast formation and patterning during early brain development in *Drosophila*. Bioessays 26, 739–751.
Vieille-Grosjean, I., Hunt, P., Gulisano, M., Boncinelli, E., Thorogood, P., 1997. Brachial Hox gene expression and human craniofacial development. Dev. Biol. 183, 49–60.
White, K., Grether, M.E., Abrams, J.M., Young, L., Farell, K., Steller, H., 1994. Genetic control of programmed cell death in *Drosophila*. Science 264, 677–683.
Wilkinson, D.G., Bhatt, S., Cook, M., Boncinelli, E., Krumlauf, R., 1989. Segmental expression of Hox-2 homeobox-containing genes in the developing mouse hindbrain. Nature 341, 405–409.
Wong, D.C., Lovick, J.K., Ngo, K.T., Borisuthirattana, W., Omoto, J.J., Hartenstein, V., 2013. Postembryonic lineages of the *Drosophila* brain: II. Identification of lineage projection patterns based on MARCM clones. Dev. Biol. 384, 258–289.
Younossi-Hartenstein, A., Nassif, C., Green, P., Hartenstein, V., 1996. Early neurogenesis of the *Drosophila* brain. J. Comp. Neurol. 370, 313–329.
Yu, H.H., Awasaki, T., Schroeder, M.D., Long, F., Yang, J.S., Ding, P., Kao, J.C., Wu, G.Y., Peng, H., Myers, G., Lee, T., 2013. Clonal development and organization of the adult *Drosophila* brain. Curr. Biol. 23, 633–643.